Japanese Journal of Radiology (2020) 38:878–883
https://doi.org/10.1007/s11604-020-00987-5

ORIGINAL ARTICLE

Improved image quality of temporal bone CT with an ultrahigh-resolution CT scanner: clinical pilot studies

Arisa Ohara[1] · Haruhiko Machida[1] · Hisae Shiga[1] · Wataru Yamamura[2] · Kenichi Yokoyama[1]

Received: 2 March 2020 / Accepted: 29 April 2020 / Published online: 11 May 2020

Abstract

Purpose Ultrahigh-resolution CT (UHRCT) with slice collimation of 0.25 mm × 160 and matrix size of 1024 × 1024 has become clinically available. We compared the image quality of temporal bone CT (TBCT) between UHRCT and conventional multidetector CT (MDCT).

Materials and methods We retrospectively enrolled 20 patients who underwent TBCT by MDCT (matrix size, 512 × 512) and subsequently by UHRCT (matrix size, 1024 × 1024). Two independent reviewers subjectively graded delineation of normal stapes, oval window, facial nerve canal, incudostapedial joint, and tympanic tegmen. We also quantified image noise in the cerebellar hemisphere. Between MDCT and UHRCT, we compared mean subjective grades using the Wilcoxon signed-rank test and the image noise using paired *t* test.

Results Grades were significantly higher with UHRCT than with MDCT for all the anatomies ($P < 0.001$), whereas noise was significantly higher with UHRCT than with MDCT ($P = 0.002$).

Conclusion For TBCT, UHRCT shows better delineation of the fine anatomical structures compared with MDCT.

Keywords Ultrahigh-resolution CT · Temporal bone CT · Image quality

Abbreviations

MDCT	Multidetector CT
UHRCT	Ultrahigh-resolution CT

Introduction

Multidetector row CT (MDCT) is a major diagnostic tool in temporal bone imaging but is sometimes limited in the delineation of fine and complex anatomical structures of the middle and inner ears [1–4]. Since March 2017, a state-of-the-art ultrahigh-resolution CT (UHRCT) scanner has been clinically available to improve in- and through-plane spatial resolution of CT images. Major features of this CT scanner include an improved detector system (minimal slice thickness, 0.25 mm; maximal channel number, 1792) and x-ray focus (smallest size, 0.4 × 0.5 mm) compared with conventional MDCT scanners. Whereas UHRCT has been reported to be clinically useful in various CT examinations, including chest CT [5, 6], coronary CT angiography [7–9], and CT of the artery of Adamkiewicz [10], few reports appear to have examined temporal bone CT [11]. Yamashita et al. [11] previously compared the delineation of fine anatomical structures on temporal bone CT between UHRCT with a 512-matrix size and conventional MDCT. A greater matrix size can improve microstructure delineation. We thus compared image qualities of temporal bone CT between UHRCT with a 1024-matrix size and conventional MDCT.

Materials and methods

Patient population

We retrospectively enrolled 132 consecutive patients who underwent routine non-contrast temporal bone CT with the UHRCT scanner between April 1, 2017 and October 31, 2017 as a follow-up study, and who had undergone CT of the same region using a conventional 64-detector CT scanner previously at our institution without any significant interval

✉ Haruhiko Machida
hmachida@ks.kyorin-u.ac.jp

[1] Department of Radiology, Kyorin University Faculty of Medicine, 6-20-2, Shinkawa, Mitaka-shi, Tokyo 181-8611, Japan

[2] Department of Radiology, Kyorin University Hospital, 6-20-2, Shinkawa, Mitaka-shi, Tokyo 181-8611, Japan

change in clinical status based on their medical records. When two or more examinations were performed with the conventional MDCT scanner, only those CT images acquired at the most recent examination were used for this study. An experienced head-and-neck radiologist with 15 years of clinical experience reviewed the axial and MPR coronal temporal bone CT images on both sides and finally included 20 non-traumatic patients (12 men, 8 women; mean age, 62 ± 23 years; age range, 11–85 years) who showed normal temporal bone by both UHRCT and conventional MDCT without intervening change on at least one side. Median interval between the two CT examinations was 13.5 months (range, 5–40 months).

This study was approved by the institutional review board at our institution. Informed consent was obtained from every patient.

CT data acquisition

We performed temporal bone CT with both the UHRCT (Aquilion Precision; Canon Medical Systems, Otawara, Tochigi, Japan) and conventional MDCT scanners (Aquilion 64; Canon Medical Systems) using a standard helical scan method, as described elsewhere [12–14]. Scan parameters for UHRCT were: tube voltage, 120 kVp; noise index, 6.5 Hounsfield Units for 2-mm thickness with filtered back-projection by automatic exposure control; number of channels, 1792; slice collimation, 0.25 mm × 160 rows; pitch factor, 0.569; rotation time, 0.75 s; and x-ray focus size, 0.4 × 0.5 mm. Scan parameters for conventional MDCT were: tube voltage, 120 kVp; tube current, 250 mA; number of channels, 896; slice collimation, 0.5 mm × 4 rows; pitch factor, 0.625; rotation time, 0.75 s; and x-ray focus size, 0.9 × 0.8 mm. With this MDCT scanner, we fixed the tube current because automatic exposure control was unavailable; and used only the central 4 rows of detectors to reduce the effect of cone angle and thus applied quarter-offset reconstruction to improve in-plane spatial resolution.

We recorded the volume CT dose index (measured in mGy) displayed on the dose report on the CT scanner for each patient and calculated the mean volume CT dose index in our patients.

Image reconstruction and display

For each patient, we used filtered back-projection to reconstruct temporal bone CT axial and MPR coronal images by both UHRCT and conventional MDCT using the following parameters: FOV, 10 cm; matrix size, 1024 × 1024; slice thickness and interval, 0.6 mm; and bone kernel, FC 80 for the UHRCT; FOV, 10 cm; matrix size, 512 × 512; slice thickness and interval, 0.6 mm; and bone kernel, FC 80 for the conventional MDCT. All CT images were transferred to a PACS (SYNAPSE; FUJIFILM Medical, Tokyo, Japan) and displayed with a window width of 4000 Hounsfield Units and window level of 600 Hounsfield Units.

Image quality assessment

Two independent radiologists with 15 (Reviewer 1) and 5 (Reviewer 2) years of clinical experience freely scrolled the temporal bone CT images on the PACS using a paging method and subjectively graded the delineation of the following high-contrast structures only on the normal side in each patient: the stapes, oval window, and tympanic segment of the facial nerve canal on axial images, and the incudostapedial joint, oval window, and tympanic tegmen on MPR coronal images. We used a 5-point scale for grading: one (poor), not visible; two (fair), partially visible; three (moderate), generally visible with slight blurring or discontinuity; four (good), clearly visible with complete continuity; and five (excellent), very clearly visible with complete continuity. These anatomical structures were selected as clinically critical, but often difficult to completely and clearly delineate with a conventional MDCT scanner. Dehiscence is known to be identified in the tympanic segment of the facial nerve canal (mostly around the oval window) and the tympanic tegmen even in normal cases [15–17]. We thus defined a subjective grade of three points or less as the presence of dehiscence in these two structures.

For quantitative assessment of image noise, we placed a circular region of interest of approximately 10 mm^2 in the cerebellar hemisphere on the same side to measure the standard deviation of the CT value as the background noise on temporal bone CT images by UHRCT and conventional MDCT in each patient.

Statistical analysis

All continuous variables are expressed as mean ± standard deviation. We performed statistical analyses using commercially available software (IBM SPSS Statistics version 23; IBM, Armonk, NY). We used the Wilcoxon signed-rank test to compare subjective image quality graded for each anatomy on the temporal bone CT axial and MPR coronal images, the McNemar test to compare the incidence of dehiscence in the tympanic segment of the facial nerve canal and the tympanic tegmen between UHRCT and conventional MDCT. We used paired *t*-test to compare quantitative image noise after confirming the normal distribution and the Wilcoxon signed-rank test to compare the mean volume CT dose index between UHRCT and conventional MDCT. Values of $P < 0.05$ were considered statistically significant. We also used weighted kappa (κ) statistics to quantify inter-reviewer agreement on subjective image quality grade. Values of κ were interpreted as follows: poor, 0.00–0.20; fair,

0.21–0.40; moderate, 0.41–0.60; good, 0.61–0.80; and excellent, 0.81–1.00.

Results

Table 1 shows average image quality grades for each anatomy by UHRCT and conventional MDCT by the two Reviewers. The grades on both axial and MPR coronal images were significantly better by UHRCT than by conventional MDCT for all the anatomies ($P < 0.001$) (Figs. 1, 2, 3, 4).

The incidence of dehiscence in the tympanic segment of the facial nerve canal and tympanic tegmen was comparable between UHRCT and conventional MDCT for Reviewer 1 ($P = 0.182$ and 0.133, respectively), although that in both anatomies was significantly lower by UHRCT than by conventional MDCT for Reviewer 2 ($P < 0.001$ and $= 0.023$, respectively) (Table 2; Figs. 1, 2, 3).

Inter-reviewer agreement of all subjective image quality scores was good ($\kappa = 0.69$).

Mean volume CT dose index was significantly lower with UHRCT (45.3 ± 2.1 mGy) than with conventional MDCT (128.2 ± 9.9 mGy; $P < 0.001$).

Quantitative noise was significantly higher by UHRCT (151.7 ± 26.2 Hounsfield Units) than by conventional MDCT (126.9 ± 17.6 Hounsfield Units; $P = 0.002$).

Discussion

UHRCT can improve in- and through-plane spatial resolution compared with conventional MDCT and achieve the maximal spatial resolution of approximately 0.15 mm, mainly due to the improved detector system and x-ray focus [5, 6]. In the present study, use of UHRCT significantly improved delineation of all high-contrast, fine, and critical anatomical structures on temporal bone CT compared with conventional MDCT. Yamashita et al. [11] demonstrated

Table 1 Average image quality grades by Reviewers 1 and 2

	UHRCT	MDCT	*P* value
Axial			
Stapes	4.8 ± 0.4	3.6 ± 0.5	< 0.001
Oval window	4.7 ± 0.5	3.6 ± 0.6	< 0.001
Facial nerve canal	4.0 ± 0.8	3.2 ± 0.6	< 0.001
Coronal			
Incudostapedial joint	4.8 ± 0.4	3.6 ± 0.5	< 0.001
Oval window	4.8 ± 0.4	3.2 ± 0.4	< 0.001
Tympanic tegmen	4.9 ± 0.3	3.9 ± 0.7	< 0.001

MDCT multidetector row CT, *UHRCT* ultrahigh-resolution CT

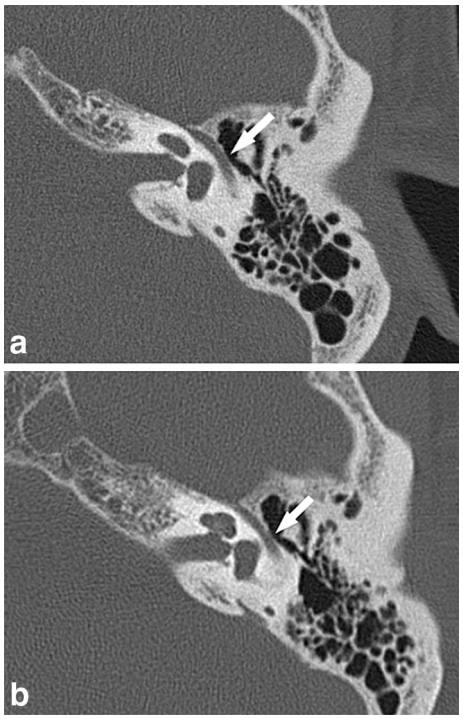

Fig. 1 Axial images of the left temporal bone CT from the same case. Image quality scores for the tympanic segment of the facial nerve canal (arrow) by Reviewers 1 and 2 are five and four, respectively, on UHRCT (**a**), and three on MDCT (**b**) by both Reviewers. By both Reviewers, dehiscence in this anatomy was considered to be present on MDCT but not on UHRCT

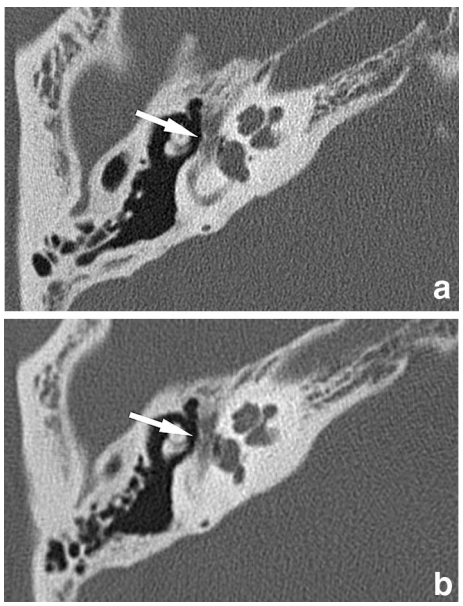

Fig. 2 Axial images of the right temporal bone CT from the same case. Image quality scores for the tympanic segment of the facial nerve canal (arrow) by Reviewers 1 and 2 are three and four on UHRCT (**a**), respectively, and two and three on MDCT (**b**). Dehiscence in this anatomy was considered to be present by both Reviewers on MDCT; only by Reviewer 1 but not by Reviewer 2 on UHRCT

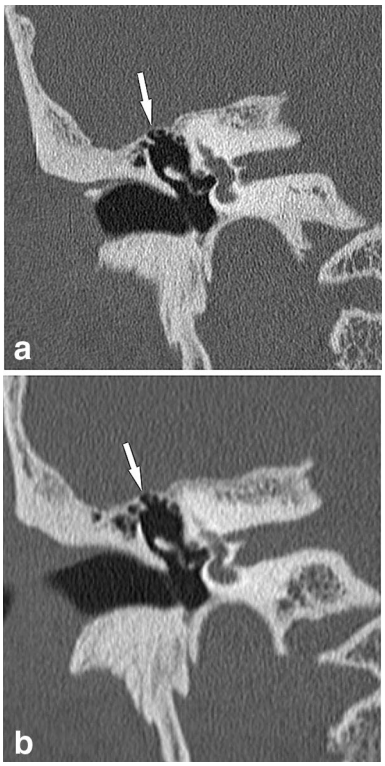

Fig. 3 Coronal images of the right temporal bone CT from the same case. Image quality scores for the tympanic tegmen (arrow) are five on UHRCT (**a**), and three on MDCT (**b**) by both Reviewers. By both Reviewers, dehiscence in this anatomy was considered to be present on MDCT but not on UHRCT

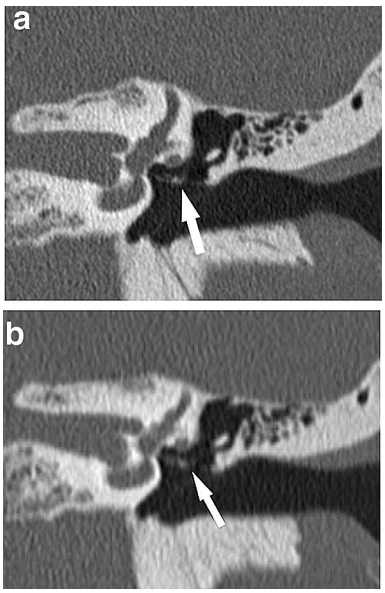

Fig. 4 Coronal images of the left temporal bone CT from the same case. Image quality scores of the incudostapedial joint (arrow) are five on UHRCT (**a**), and three on MDCT (**b**) by both Reviewers

that only the stapedius tendon was more clearly visualized on temporal bone CT by UHRCT than by 320-detector CT. However, all other anatomical structures were similarly visualized between both, possibly due to the use of a 512-matrix size also for UHRCT, different from the situation in our study (i.e., 1024-matrix size).

Dehiscence is known to be identified in the facial nerve canal and tympanic tegmen even in normal cases [15–17]. The incidence of dehiscence of both the facial nerve canal and tympanic tegmen was higher by conventional MDCT than by UHRCT, although not significantly for Reviewer 1, possibly resulting from a greater partial volume effect due to lower spatial resolution in conventional MDCT. According to published data from cadaveric and surgical studies [15, 18–21], the incidence of facial nerve canal dehiscence ranged from 25 to 74%. According to published data from cadaveric studies, the incidence of tympanic tegmen dehiscence was reported as 20% [16, 17]. Thus, dehiscence of both the facial nerve canal and tympanic tegmen might have been overestimated by Reviewer 2 using conventional MDCT alone, as that Reviewer had less experience with temporal bone CT interpretation.

We performed helical scanning and reconstructed 0.6-mm-slice images by filtered back-projection as per our clinical routine examinations. Use of axial or volume scanning for decreasing artifacts related to helical scanning and a thinner slice thickness for improving spatial resolution, if necessary, without increasing image noise by hybrid or model-based iterative reconstruction can not only further improve delineation of the aforementioned structures and diagnostic accuracy of the dehiscence of both the anatomies, but can also achieve visualization of more subtle structures such as mucosal folds of the middle ear.

Mean volume CT dose index by conventional MDCT without using automatic exposure control (tube current-exposure time product: 187.5 mAs) was lower than that in previous studies [1, 11], but significantly higher than that by UHRCT in our study. Mean volume CT dose index by conventional MDCT was higher, but that by UHRCT was lower than the diagnostic reference levels for head CT (56–85 mGy) in the United States, European countries, and Japan [22–24]. Use of axial or volume scanning and hybrid or model-based iterative reconstruction may further reasonably reduce radiation dose by UHRCT. Whereas quantitative image noise was greater by UHRCT with better spatial resolution than by conventional MDCT, the use of the iterative reconstruction can also reduce the noise.

Our study was limited in the retrospective design and inclusion of only a small study population from a single institution. We only used the single scan and reconstruction protocol for temporal bone CT. Use of different scan and reconstruction protocols may affect the study results. The diagnosis of dehiscence of the facial nerve canal and

Table 2 Presence of dehiscence on CT

Reviewer 1	UHRCT	MDCT	*P* value
Facial nerve canal	7/20 (35%)	12/20 (60%)	0.182
Tympanic tegmen	0/20 (0%)	4/20 (20%)	0.133
Reviewer 2	UHRCT	MDCT	*P* value
Facial nerve canal	5/20 (25%)	19/20 (95%)	< 0.001
Tympanic tegmen	0/20 (0%)	7/20 (35%)	0.023

MDCT multidetector row CT, *UHRCT* ultrahigh-resolution CT

the tympanic tegmen by temporal bone CT was not surgically confirmed. Intervals between conventional MDCT and UHRCT examinations were long (median, 13.5 months) due to the retrospective nature of the study, although shorter-interval examinations would not be practical due to the increased radiation exposure. Although we only evaluated the delineation of normal anatomical structures on temporal bone CT, further studies are needed to assess diagnostic performance for middle ear diseases such as cholesteatoma and otosclerosis. However, a comparison of diagnostic performance between conventional MDCT and UHRCT in the same patients is challenging, as these diseases are likely to change over time.

In conclusion, the latest UHRCT increases image noise but appears useful by offering sharper, clearer, more continuous delineation of fine anatomical structures in routine temporal bone CT scanning with higher spatial resolution compared with conventional MDCT. These benefits are mainly due to the improved detector system and x-ray focus.

Acknowledgements We thank Ms. Mika Tsuboi (Canon Medical Systems) for her comments of the manuscript.

Funding This work was supported by a Grant-in-Aid for Scientific Research (C) 18K07643 from the Japan Society for the Promotion of Science, Japan.

References

1. Leng S, Diehn FE, Lane JI, Koeller KK, Witte RJ, Carter RE, et al. Temporal bone CT: Improved image quality and potential for decreased radiation dose using an ultra-high-resolution scan mode with an iterative reconstruction algorithm. AJNR Am J Neuroradiol. 2015;36:1599–603.
2. Jäger L, Bonell H, Liebl M, Srivastav S, Arbusow V, Hempel M, et al. CT of the normal temporal bone: comparison of multi- and single-detector row CT. Radiology. 2005;235:133–41.
3. Lane JI, Lindell EL, Witte RJ, DeLone DR, Driscoll CLW. Middle and inner ear: improved depiction with multiplanar reconstruction of volumetric CT data. Radiographics. 2006;26:115–24.
4. Chuang MT, Chiang IC, Lin WC. Multidetector row CT demonstration of inner and middle ear structures. Clin Anat. 2006;19:337–44.
5. Kakinuma R, Moriyama N, Muramatsu Y, Gomi S, Suzuki M, Nagasawa H, et al. Ultra-high-resolution computed tomography of the lung: image quality of a prototype scanner. PLoS ONE. 2015;10(9):e0137165. https://doi.org/10.1371/journal.pone.0137165.
6. Hata A, Yanagawa M, Honda O, Kikuchi N, Miyata T, Tsukagoshi S, et al. Effect of matrix size on the image quality of ultra-high-resolution ct of the lung: comparison of 512 × 512, 1024 × 1024, and 2048 × 2048. Acad Radiol. 2018;25:869–76.
7. Takagi H, Tanaka R, Nagata K, Ninomiya R, Arakita K, Schuijf JD, et al. Diagnostic performance of coronary CT angiography with ultra-high-resolution CT: Comparison with invasive coronary angiography. Eur J Radiol. 2018;101:30–7.
8. Pontone G, Bertella E, Mushtaq S, Loguercio M, Cortinovis S, Baggiano A, et al. Coronary artery disease: diagnostic accuracy of CT coronary angiography-a comparison of high and standard spatial resolution scanning. Radiology. 2014;271:688–94.
9. Andreini D, Pontone G, Mushtaq S, Conte E, Perchinunno M, Guglielmo M, et al. Atrial fibrillation: diagnostic accuracy of coronary CT angiography performed with a whole-heart 230-µm spatial resolution CT scanner. Radiology. 2017;284:676–84.
10. Yoshioka K, Tanaka R, Takagi H, Ueyama Y, Kikuchi K, Chiba T, et al. Ultra-high-resolution CT angiography of the artery of Adamkiewicz: a feasibility study. Neuroradiology. 2018;60:109–15.
11. Yamashita K, Hiwatashi A, Togao O, Kikuchi K, Matsumoto N, Momosaka D, et al. Ultrahigh-resolution CT scan of the temporal bone. Eur Arch Otorhinolaryngol. 2018;275:2797–803. https://doi.org/10.1007/s00405-018-5101-6.
12. Klingebiel R, Bauknecht HC, Rogalla P, Bockmühl U, Kaschke O, Werbs M, et al. High-resolution petrous bone imaging using multi-slice computerized tomography. Acta Otolaryngol. 2001;121:632–6.
13. Venema HW, Phoa SS, Mirck PG, Hulsmans FJ, Majoie CB, Verbeeten B. Petrous bone: coronal reconstruction from axial spiral

data obtained with 0.5-mm collimation can replace direct coronal sequential CT scans. Radiology. 1999;213:375–82.
14. Fujii N, Inui Y, Katada K. Temporal bone anatomy: correlation of multiplanar reconstruction sections and three-dimensional computed tomography images. Jpn J Radiol. 2010;28:637–48.
15. Takahashi H, Sando I. Facial canal dehiscence: histologic study and computer reconstruction. Ann Otol Rhinol Laryngol. 1992;101:925–30.
16. Kapur TR, Bangash W. Tegmental and petromastoid defects in the temporal bone. J Laryngol Otol. 1986;100:1129–32.
17. Lang DV. Macroscopic bony deficiency of the tegmen tympani in adult temporal bones. J Laryngol Otol. 1983;97:685–8.
18. Beddard D, Saunders WH. Congenital defects in the fallopian canal. Laryngoscope. 1962;72:112–5.
19. Dimopoulos PA, Muren C, Smedby Ö, Wadin K. Anatomical variations of the tympanic and mastoid portions of the facial nerve canal. Acta Radiol. 1996;403:49–59.
20. Baxter A. Dehiscence of the fallopian canal. an anatomical study. J Laryngol Otol. 1971;85:587–94.
21. Fuse T, Tada Y, Aoyagi M, Sugai Y. CT detection of facial nerve canal dehiscence and semicircular canal fistula: comparison with surgical findings. J Comput Assist Tomogr. 1996;20:221–4.
22. Diagnostic reference levels based on latest surveys in Japan—Japan DRLs 2015—. Japanese Network for Research and Information on Medical Exposure. Available at: https://www.radher.jp/J-RIME/report/DRLhoukokushoEng.pdf.published2015. Accessed 10 July 2018
23. Kanal KM, Butler PF, Sengupta D, Bhargavan-Chatfield M, Coombs LP, Morin RL. U.S. diagnostic reference levels and achievable doses for 10 adult CT examinations. Radiology. 2017;284:120–33.
24. European Commission (EC). Radiation Protection No.180-Diagnostic reference levels in thirty-six European countries (Part 2/2). EC website. Published 2014. Available at: https://ec.europa.eu/energy/sites/ener/files/documents/RP180%20part2.pdf. Accessed 10 July 2018